Composite Structures 321 (2023) 117304

Contents lists available at ScienceDirect

Composite Structures

journal homepage: www.elsevier.com/locate/compstruct

In-situ aligning magnetic nanoparticles in thermoplastic adhesives for contactless rapid joining of composite structures

Zhao Sha [a], Xinying Cheng [a,b], Andrew D.M. Charles [c], Yang Zhou [a], Mohammad S. Islam [a], Andrew N. Rider [c], Shuhua Peng [a], May Lim [d], Victoria Timchenko [a], Chun H. Wang [a,*]

[a] School of Mechanical and Manufacturing Engineering, University of New South Wales, Sydney, NSW 2052, Australia
[b] Institute of Photonics, Leibniz University Hannover, Hannover 30167, Germany
[c] Defence Science and Technology Group, 506 Lorimer Street, Fisherman's Bend, VIC 3207, Australia
[d] School of Chemical Engineering, University of New South Wales, Sydney, NSW 2052, Australia

ARTICLE INFO

Keywords:
Magnetic aligning
Thermoplastic adhesive
Iron oxide nanoparticle
Magnetic hysteresis loss
Inductive heating

ABSTRACT

Magnetic nanoparticles of high magnetic susceptibility, such as magnetite (Fe_3O_4), have been used for wireless heating of adhesives and composites through the magnetic hysteresis loss mechanism, but the high concentrations of nanoparticles needed to meet heating performance targets can degrade mechanical properties. Herein, we present an in-situ aligning method to enhance the heating efficiency of magnetite nanoparticles in a nylon thermoplastic matrix without adversely affecting its mechanical strength. A composite adhesive was made by dispersing Fe_3O_4 nanoparticles in a nylon matrix followed by hot melting. Experimental results show that by subjecting the adhesive to an alternating magnetic field during the hot-melt process, its heating rate can be improved by 200% compared to that without applying the magnetic field. The improvement in the heating performance has been identified to stem from the alignment of the ease axis of the magnetic nanoparticles. This in-situ aligning technique enables better induction heating performance with the same amount of Fe_3O_4 nanoparticles, avoiding the agglomeration problem of high nanoparticle concentrations. Moreover, this technique makes it possible to develop high-performance self-heating thermoplastic adhesive for reversible bonding and self-healing solution with a wide range of applications, such as bonding and debonding of composites, temporary attachment of systems, and recyclable bonded structures.

1. Introduction

Rapid joining and disassembly of composite structures hold great potential for the widening application and recyclability of composites [1,2]. However, connecting components with traditional mechanical fasteners (e.g. bolts, rivets, screws) can cause issues like stress concentrations and fibre cut due to drilling operation, which largely reduce the strength and service endurance of the components [3,4,5,6,7]. One promising solution to these issues is to deploy reversible adhesive bonding, especially in situations where traditional mechanical fasteners are not suitable [8,9]. Unlike permanent bonding by thermosetting adhesives, reversible adhesive bonding provides the possibility of easy replacement and disassembly of composite components, better recyclability, and thus lower cost [10,11]. Besides, the bonded joints generally have a good resistance to fatigue, especially with thermoplastic adhesives that may have toughness higher than thermosetting adhesives [12,13,14].

To date, multiple thermoplastic polymers, such as poly(ethylene-methacrylic acid) (EMAA) [15], polyolefin [16,17], ethylene vinyl acetate (EVA) [18], poly(ethylene-co-butylene) [19], polyurethane (PU) [20], APOA/Polyolefin ester [21], natural rubber [22], and acrylonitrile butadiene styrene (ABS) [23], have been applied as reversible adhesives to bond composites components. The hot-melt feature of these thermoplastic polymers enables a convenient disassembly and reconnection of different components by applying certain heat and force [24,25]. However, limited by the relatively low bonding strength and temperature capabilities, most of the thermoplastic polymer adhesives mentioned above are not suitable for structures requiring high strength and higher operating temperatures. Therefore, it is of great importance to develop new solutions to enable reversible adhesive bonding with high bond strength and wide operating temperature range.

In addition to choosing the right thermoplastic polymer as the

* Corresponding author.
E-mail address: chun.h.wang@unsw.edu.au (C.H. Wang).

https://doi.org/10.1016/j.compstruct.2023.117304
Received 24 December 2022; Received in revised form 5 May 2023; Accepted 22 June 2023
Available online 24 June 2023

adhesive, the appropriate heating method is also crucial for the application of reversible bonding technique. A successful reversible bonding technique involves two key processes: bonding and debonding. For the bonding process, the thermoplastic adhesive has to be first heated to molten state, then it solidifies upon cooling, and the two surfaces are joined. While the debonding process is achieved by applying heat to melt the adhesive again, allowing the two surfaces to separate. Lee et al. [9] developed a thermoplastic adhesive film that was stitched by stainless steel fibres. The adhesive film can be melted with the Joule heat generated by stainless steel fibres, thus achieving the on-demand bonding and debonding. However, this method requires external wiring as well as a current loop inside the adhesive, which limit its application in some complex structures and hard-to-access areas. Electromagnetic induction heating shows great potential to achieve a contactless and localized heating of adhesives [26], avoiding some of the major limitations of conventional methods (e.g. hot glue gun, heating blankets or IR lamps), such as overheating of the surrounding structures [15,27,28] and reaching hard-to-access areas [29]. Incorporation of ferrimagnetic materials, which exhibit a magnetic hysteresis loss mechanism under an alternating magnetic field, can enable contactless and localized heating of thermoplastic adhesives through electromagnetic induction. By using this method, several thermoplastic adhesives capable of self-heating under alternating magnetic field have been developed, including EMAA/Fe_3O_4 adhesive [15], PU/Fe_3O_4 adhesive [20], and polypropylene/Fe_3O_4 adhesive [30]. These thermoplastic adhesives can be heated to above their melting point through electromagnetic induction, thus enabling a reversible and contactless on-demand bonding and debonding of components. However, these existing studies have some major shortcomings, such as relatively low melting point of the selected adhesives, moderate bonding strengths, as well as a trade-off between the adhesive's heating rate and bonding strength, which in turn limit their applications.

In our recent work [15], EMAA and Fe_3O_4 nanoparticles were combined to develop an adhesive that can be heated under alternating magnetic field. Although the heating rate and bonding strength of adhesive have been improved by optimizing the ratio of EMAA and Fe_3O_4 nanoparticles, the adhesive was only able to achieve a heating rate of about 0.4 °C/s (20 wt% Fe_3O_4, 189 kHz, 250A current), and bonding strength of about 8.2 MPa (5 wt% Fe_3O_4), which is significantly lower than common structural adhesives. Besides, the melting temperature of EMAA is only about 76 °C, limiting it to applications where the operating temperature is lower than its melting temperature. However, selecting a thermoplastic polymer with a higher melting temperature requires longer heating time and potentially much higher concentration of magnetic nanoparticles that can then adversely affect the bond strength.

Herein, we present a novel composite adhesive that is made of Nylon 12 polymer and Fe_3O_4 nanoparticles. The Nylon 12 has a high melting point of approximately 178 °C as well as a good bonding strength, making it suitable as a structural adhesive. Unlike being random dispersed as they were in the aforementioned studies, a magnetic field was applied to the melted nanocomposite adhesive to align the ease axis of the Fe_3O_4 nanoparticles to the magnetic flux direction during the hot-melt process, resulting in a higher imaginary part of the relative permeability μ‟ of the adhesive as well as a higher induction heating efficiency. With this in-situ alignment technique, it is possible to achieve better inductive heating performance without using excessive Fe_3O_4 nanoparticles that can result in agglomeration of nanoparticles and degradation of the bond strength of the adhesive. The alignment of ferrimagnetic nanomaterials in this study provides a new technique to develop high-performance self-heating thermoplastic composite for reversible bonding and self-healing solution for a wide range of applications, such as bonding and debonding of composites, temporary attachment of systems, and recyclable bonded structures.

2. Experimental section

2.1. Preparation of nylon 12 adhesives with Fe_3O_4 nanoparticles

Polylauryllactam (Nylon 12, Sigma-Aldrich) pellets with melting temperature of 178 °C was selected as the reversible adhesive material. Iron (II, III) oxide nanoparticles (Fe_3O_4, Sigma-Aldrich) with sizes between 50 and 100 nm were used as the dual-functional fillers for inductive heating and structural reinforcement of the adhesive. The Nylon/Fe_3O_4 adhesive films were fabricated through a similar method as described in ref [15]. Briefly, Nylon 12 pellets were ground into a powder with an average particle diameter of 250 μm. Different weight percentages of Fe_3O_4 nanoparticles were mixed with Nylon 12 powder at room temperature using a high-speed mixer (FlackTek SpeedMixer). During the high-speed mixing process, Fe_3O_4 nanoparticles were coated on the surface of Nylon 12 particle with the assistance of Coulomb's force. The resultant mixture was thermoformed into adhesive films with a thickness of 0.3 mm using a hot press under a pressure of about 6894.8 kPa (1000 psi) at 200 °C for 10 mins.

2.2. In-situ aligning of Fe_3O_4 nanoparticles in Nylon/Fe_3O_4 adhesives

The Nylon/Fe_3O_4 adhesive films were sandwiched between two glass fibre-reinforced polymer (GFRP) laminates (2 mm thickness) and placed on top of a spiral induction coil. The GFRP laminate is larger in size than the internal diameter of the spiral coil, serving both as a support for the adhesive film and to control the distance between the adhesive and the coil. To prevent the adhesive film from sticking to the GFRP laminates, PTFE films were added between the laminates and the adhesive. An observation hole with a diameter of 4 mm was drilled on the top GFRP laminate to allow the temperature monitoring of the adhesive film using an IR camera. A heat gun was used to increase the temperature of the adhesive to above its melting point. The electromagnetic aligning of Fe_3O_4 nanoparticles started by applying alternating magnetic field for 2 mins for each aligning cycle through an induction system (Ambrell, USA) when the temperature of adhesive film reached 200 °C. In this study, the aligning of Fe_3O_4 nanoparticles in the adhesive was conducted to up to 3 cycles, and the inductive heating performance of adhesive was measured after each aligning cycle to monitor the changes due to the nanoparticle alignment. The magnetisation of the nylon adhesive film before and after aligning were measured through a vibrating sample magnetometer (VSM, 8607 series, Lake Shore Cryotronics, USA) at room temperature, and the influence of alternating magnetic aligning was investigated.

2.3. Characterization of electromagnetic inductive heating

An alternating magnetic field was generated using an EASYHEAT induction heating system (Ambrell, USA) at 189 kHz operating frequency. This operating frequency is automatically selected by the induction heating system as the optimum working frequency, which is determined by the composition and dimension of the samples. The axial length of the spiral coil was 32 mm with eight turns. Its inner and outer diameters measured 24 mm and 38 mm, respectively. The coil was of a hollow configuration, which enabled the inflow of water to facilitate cooling during the induction heating process. Different currents could be applied to generate magnetic flux of varying intensities up to 0.07 T. The maximum power generated by the equipment was 2.4 kW. The temperature distribution of heated adhesive was measured using an infrared camera (FLIR X6540sc), and 3 samples were measured per each group.

2.4. Characterization of adhesive strength

The bond strength of the Nylon/Fe_3O_4 adhesive was measured using a tensile lap-shear test at room temperature. Two adherends made of unidirectional carbon fibre (UniCF) reinforced epoxy laminates (25 mm

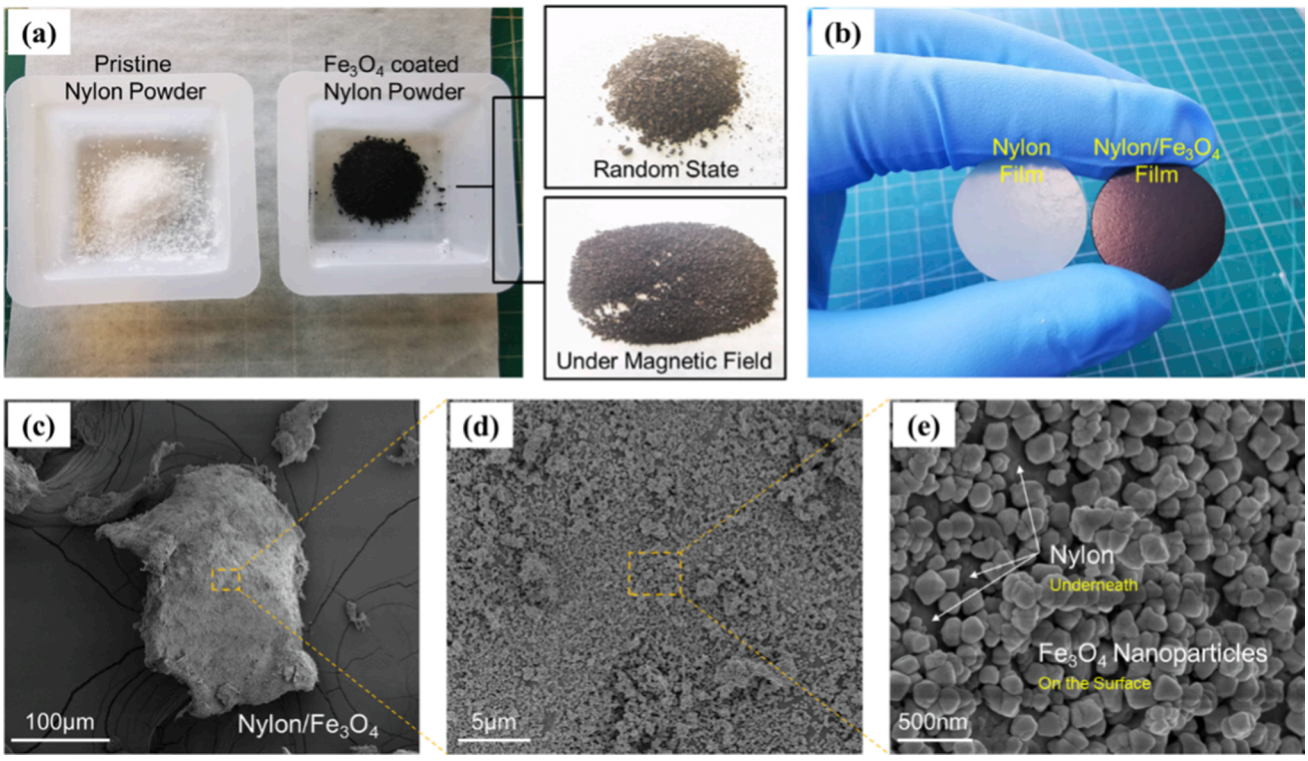

Fig. 1. Morphologies of nylon microparticles before and after coating of iron oxide nanoparticles: (a) digital image of pristine and iron oxides coated nylon powder; (b) digital image of nylon film and nylon/Fe_3O_4 film; (c) SEM image of a nylon particle coated with iron oxide nanoparticles; (d) A enlarged view of the iron oxide nanoparticles coated nylon surface; and (e) SEM image of iron oxide nanoparticles coated on the nylon surface.

× 50 mm × 1.6 mm, CF volume fraction: 50%~60%) were bonded with the Fe_3O_4-containing Nylon adhesive with an overlap area of 25 mm × 12.5 mm. An Instron 3369 universal testing machine with a 10kN load cell was used for the adhesive strength tests using a crosshead displacement rate of 1 mm/min, according to ASTM D3165. The lap-shear strength was calculated from the tensile force per unit overlap area, and 3 samples were tested per each group.

3. Results and discussion

3.1. Morphologies

The morphologies of pristine nylon powder and iron oxide coated nylon powder were observed prior to conducting the hot-pressing procedure, as shown in Fig. 1a. It can be clearly seen that after the high-speed mixing, the nylon particles were coated with iron oxide nanoparticles, and the colour of nylon powder changed from white to dark black.

Meanwhile, it was observed that with the iron oxide coating, these nylon particles can respond to the external magnetic field and rotate to align their ease axis to the external magnetic field. A scanning electron microscope (FEI Nova NanoSEM 450) was used to characterize the surface morphology of the Fe_3O_4-coated Nylon particles. Fig. 1c shows a SEM image of one nylon particle coated with iron oxide nanoparticles. The nylon particles are generally with a size around 200 ~ 300 μm, and after the high-speed mixing procedure, millions of iron oxide nanoparticles were successfully coated on their surface, as shown in Fig. 1d. These iron oxide nanoparticles are nearly ellipsoidal shaped with sizes between 50 ~ 150 nm, as can be seen in Fig. 1e. After the hot pressing, nylon adhesive films reached a typical thickness of 0.3 mm. Fig. 1b shows a typical nylon/ Fe_3O_4 adhesive film sample applied in this study, for comparison, a pristine nylon film fabricated through the same

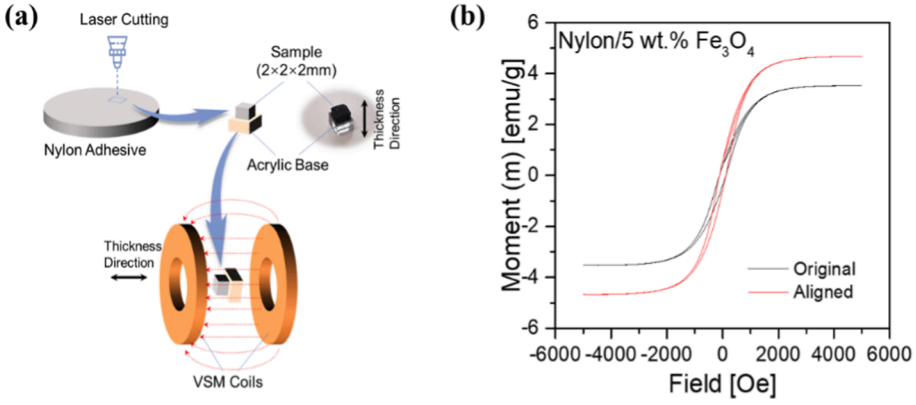

Fig. 2. VSM results: (a) Schematic of the VSM sample preparation and measurement; (b) The magnetic moment curve of original and aligned nylon/5 wt% Fe_3O_4 adhesive.

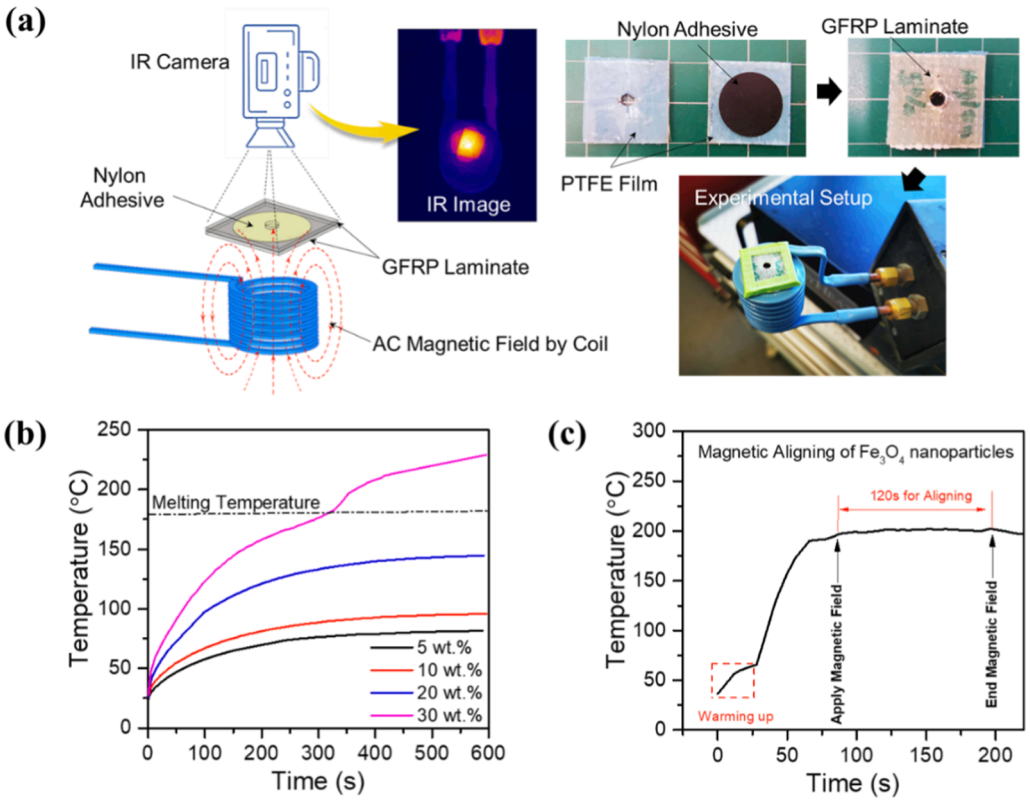

Fig. 3. Induction heating performance results: (a) Schematic of the induction heating process, and photos of experimental sample and setup; (b) Temperature changes of nylon adhesives with different iron oxide mass loadings during the induction heating; (c) Temperature changes of nylon adhesives during the iron oxides aligning process.

process is also presented.

3.2. Vibrating-sample magnetometry measurement

Under an alternating magnetic fields iron oxide nanoparticles can rotate in a liquid. However, due to their near-ellipsoidal shape and small size, it is difficult to directly observe the rotation of nanoparticles. Two micro-CT images about the cross-section view of original and aligned nylon/Fe_3O_4 adhesive are shown in Fig.S1. These images allow for a rough observation of the potential chaining of iron oxide nanoparticles, which may be attributed to the alignment process achieved via exposure to an alternating magnetic field. A qualitative analysis was conducted with vibrating-sample magnetometry (VSM) to investigate the changes in the magnetisation of the nylon/Fe_3O_4 adhesive before and after the alternating magnetic field alignment. Adhesive film for VSM measurements was prepared with larger thickness (2 mm) to meet the sample requirement, and its iron oxide mass loading was selected to be 5 wt%. Alignment by alternating magnetic field was conducted through the thickness direction of adhesive after the temperature was heated to above the melting point of nylon. To ensure that the adhesive film maintained its flat surface for the VSM measurement, a shorter aligning duration of around 15 s was chosen for the VSM sample, unlike the normal aligning duration of 120 s for thin film samples. After the magnetic aligning, cubic samples measuring $2 \times 2 \times 2$ mm^3 were cut from the nylon/Fe_3O_4 adhesive with a CO_2 laser engraver (Speedy 360, Trotec, Austria). The cubic samples were then bonded to acrylic blocks to assist with clamping in the VSM. Fig. 2a shows a schematic of the VSM sample preparation and measurement. For comparison, a VSM sample was prepared in the same way for the non-aligned original nylon/5 wt% Fe_3O_4 adhesive. During the measurement, the applied magnetic field was swept from −5000 Oe to 5000 Oe, and the magnetisation of the sample was recorded. Fig. 2b shows a comparison of the adhesive's magnetic dipole moment response to the applied field before and after magnetic aligning. In both cases, a hysteresis is observed in the response, typical of ferri- and ferromagnetic materials. Furthermore, the saturation magnetization, measured as the maximum magnetic moment, is enhanced by approximately 33% in the magnetically aligned sample, with a value of 4.67 emu/g, compared to the original sample which has a value of 3.52 emu/g. It is noted that the saturation magnetization of the aligned sample is similar in value when measured in direction that is perpendicular to or parallel to the alternating magnetic field, as shown in Fig.S2. This change in the overall response of the nanocomposite would lead to higher energy dissipations during the induction heating process [31] as well as an improved induction heating performance.

3.3. Induction heating performance

The nanocomposite adhesive films were sandwiched between two glass fibre-reinforced polymer (GFRP) laminates (2 mm thickness) and placed on top of a spiral induction coil. The induction heating of these adhesive films was achieved under an alternating magnetic field (189 kHz, 300A induction current). A small hole was drilled into the top laminate to assist temperature monitoring through an IR camera, the schematic of test setup as well as digital images of experimental sample and setup are shown in Fig. 3a. The temperature data within the small hole area were recorded to evaluate the induction heating performance of the nanocomposite adhesives. To begin with, the heating performance of the adhesives containing 5 wt% to 30 wt% iron oxides were measured, as shown in Fig. 3b. It can be observed that with the increase of iron oxide mass loading, both the initial heating rate and the stable temperature of adhesive can be improved. However, even under an induction current of 300 A, only the adhesive with the highest iron oxide mass loading (30 wt%) can be heated to above the melting temperature of nylon. In addition, as can be observed from the temperature change

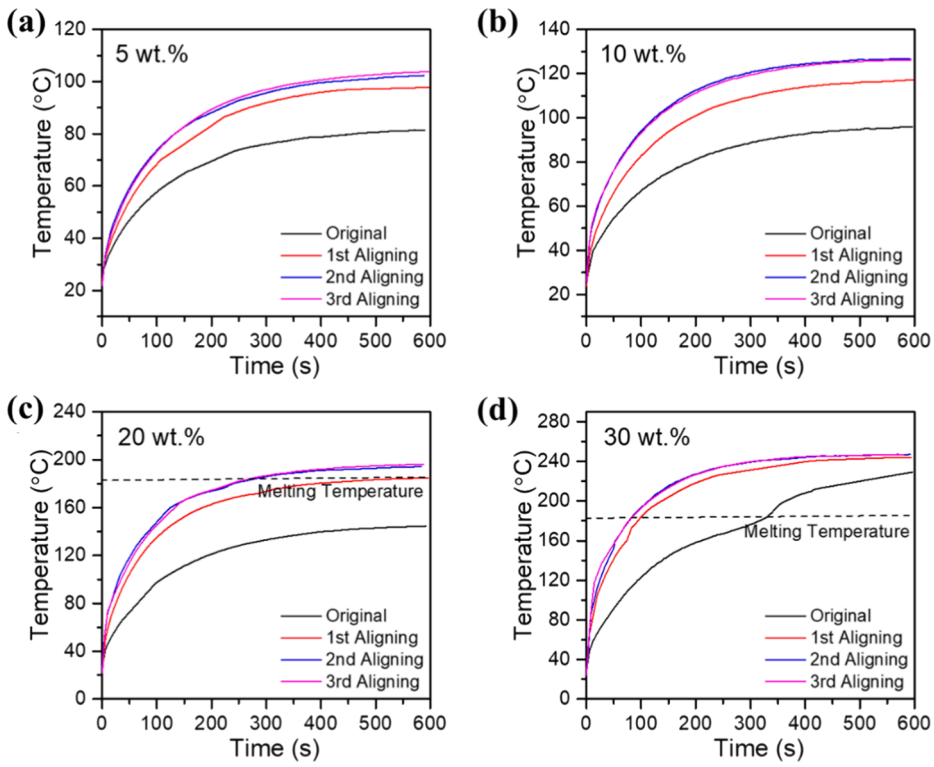

Fig. 4. Induction heating performance of nylon adhesives with (a) 5 wt%, (b) 10 wt%, (c) 20 wt% and (d) 30 wt% iron oxide before and after the magnetic aligning process.

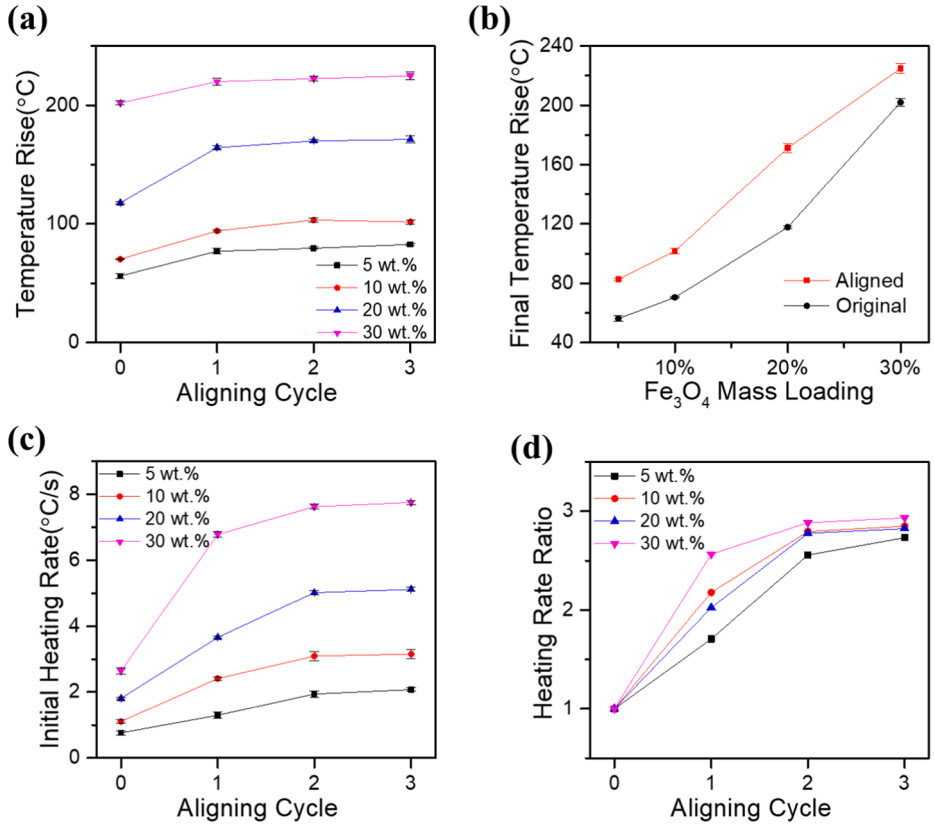

Fig. 5. Induction heating performance: (a) Plot of temperature rise against the number of aligning cycles; (b) A comparison of final temperature rises before and after magnetic aligning among adhesives with different iron oxides mass loadings; (c) Plot of initial heating rate against the number of aligning cycles; (d) Plot of initial heating rate increasing ratio against the number of aligning cycles.

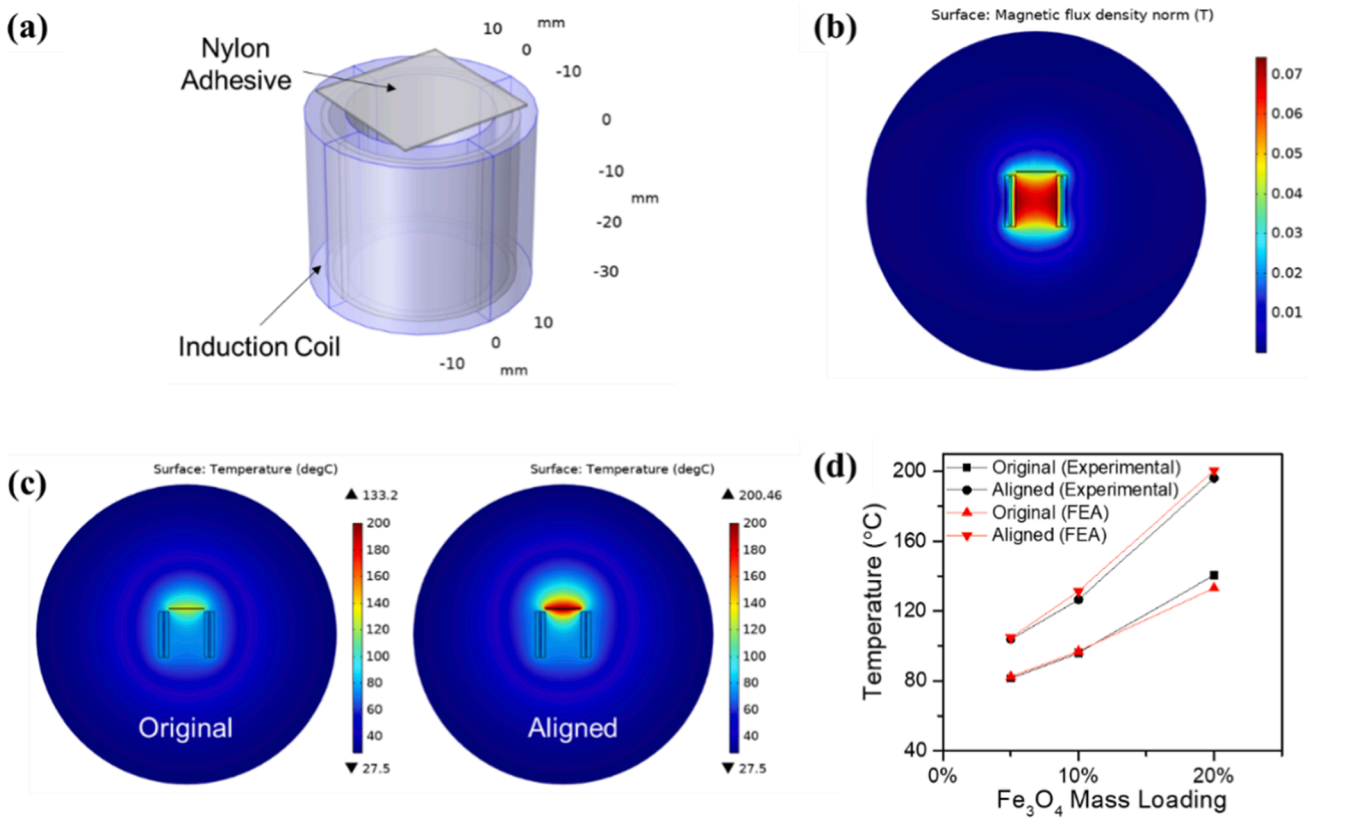

Fig. 6. FEA results: (a) Model geometry; (b) Magnetic flux distribution under an induction current of 300A; (c) Stable temperature of Nylon/20 wt% Fe_3O_4 adhesive before and after magnetic aligning; (d) Comparison between experimental and FEA results.

curve, when the adhesive was heated over its melting temperature, there was a temporarily increase in terms of the heating rate.

To improve the induction heating performance, an in-situ alignment process was developed to align the magnetic nanoparticles, as shown in Fig. 3c. The adhesives were firstly heated to ~ 200 °C (above the melting temperature of nylon) by a heat gun, then an alternating magnetic field was deployed to align the iron oxide nanoparticles inside the adhesive. A single aligning cycle lasted for 120 s and while the temperature of the adhesives was kept at 200 °C. For each group of adhesives, up to three alignment cycles were conducted with the induction heating performance of adhesive being measured after each aligning cycle. It is noted that the selection of exposure time and aligning cycles may vary as it is one of the options to align iron oxide nanoparticles in the adhesive to the saturation state. As long as these nanoparticles could be aligned to the saturation state, the resulting improvement in induction heating performance, in terms of final temperature rise and initial heating rate, are expected to be similar at the given working frequency and magnetic field intensity.

The induction heating performance of different nanocomposite adhesives after aligning are shown in Fig. 4. In general, the induction heating performance of all samples was improved after the magnetic field aligning process. The largest increase occurred after the first aligning cycle, with subsequent cycles yielding smaller increases, specifically after the second aligning cycle. After three cycles of alignment, the nanocomposite adhesives containing 5 wt% and 10 wt% magnetic nanoparticles reached a plateau temperature at about 104 °C and 127 °C, respectively. At 20 wt% concentration of magnetic nanoparticles, the peak temperature improved from 140 °C to 185 °C, reaching the melting temperature of nylon, as shown in Fig. 4c. The stable temperature of the adhesives increased slightly after the second and third aligning cycles, reaching 194.5 °C and 196 °C, respectively. Meanwhile, it is observable that the duration required for the adhesive to be heated to its melting temperature (178 °C) is significantly reduced. For the original nylon/20 wt% Fe_3O_4 adhesive, the melting temperature cannot be reached even after being heated for over 600 s. However, after the initial alignment, the adhesive requires approximately 356 s to be heated above its fusion temperature. Following the second and third alignments, this period is further reduced to around 328 and 321 s, respectively. Similar phenomenon can be observed in the heating performance of nanocomposite adhesive with 30 wt% magnetic nanoparticles. In this case the nanocomposite adhesive can be heated to above the melting point without any magnetic alignment, although the heating rate over the melting temperature increased due to the induced alignment, as shown in Fig. 4d. With these magnetic alignments, the duration required for nylon/30 wt% Fe_3O_4 adhesive to be heated to its melting temperature reduced from 316 s to about 92 s.

The temperature rises of different nanocomposite adhesives against the number of aligning cycles are plotted in Fig. 5a to illustrate the aligning effect. It can be clearly seen that for all adhesives, two magnetic aligning cycles are sufficient to achieve maximum performance. It has been reported that magnetic nanoparticles tend to have a higher imaginary part of the relative permeability when in a liquid phase substrate compared to a solid phase substrate, and this improvement is dependent on the frequency and magnetic field intensity [32]. The higher imaginary part of the relative permeability results in increased energy dissipation through hysteresis loss, leading to improved temperature rise. After two aligning cycles, it is believed that the increase in imaginary part of the relative permeability has reached a saturation state, resulting in no significant further improvement in the temperature rise. A comparison of the final temperature rises before and after magnetic aligning among adhesives with different magnetic nanoparticle loadings is shown in Fig. 5b. Among all groups of adhesives, the sample with 20 wt % magnetic nanoparticles demonstrated the largest improvement in peak temperature by 53.5 °C.

Table 1
Properties of Nylon/Fe_3O_4 adhesive for FE modelling.

Fe_3O_4 Wt.%	5%	10%	20%
Fe_3O_4 Vol.%	1%	2.1%	4.6%
μ“	6.03×10^{-4}	1.26×10^{-3}	2.76×10^{-3}
Heating Rate Ratio γ	2.73	2.85	2.82
ρ (g/cm^3)	1.052	1.099	1.204
c (J/g•K)	2.086	2.072	2.034
k (w/m•K)	0.288	0.352	0.497

The initial heating rates of adhesives were obtained by linear fitting of the initial ten-second heating curves. Improvements in the initial heating rate of adhesive after magnetic alignment can be observed from the induction heating results as well, as shown in Fig. 5c. The initial heating rates of all adhesives approached their respective maximum value after two aligning cycles. For samples with concentration of magnetic nanoparticles (5 wt%, 10 wt% and 20 wt%) the first two aligning cycles produced similar improvements in the initial heating rates, the first aligning cycle resulted the most significant increase for the high concentration (30 wt%) case, attributed to concurrent alignment during the tests. These phenomena confirm that importance of the solid–liquid phase transition of the adhesive above the melting point to the alignment of magnetic nanoparticles. The results also show that after three cycles of aligning operation all the initial heating rates increased by around 2.73 ~ 2.94, as shown in Fig. 5d, in which the heating rate ratio γ in Y axis is defined as follows.

$$\gamma = \frac{k}{k_0} \tag{1}$$

where k represents the initial heating rate of adhesive, and k_o represents the initial heating rate of unaligned adhesive. It is well-known that the relative permeability of magnetic materials consists of two parts: a real part (μ') and an imaginary part (μ“). The imaginary part (μ") will directly affect the hysteresis loss and initial heating rate of the magnetic material, which will be discussed in detail in the following section. Here, these improvements in the adhesives' initial heating rate are more likely due to the three-fold increase in imaginary part (μ“) of the relative permeability, which is estimated based on the results reported by ref. [32] at similar level of magnetic field intensity and

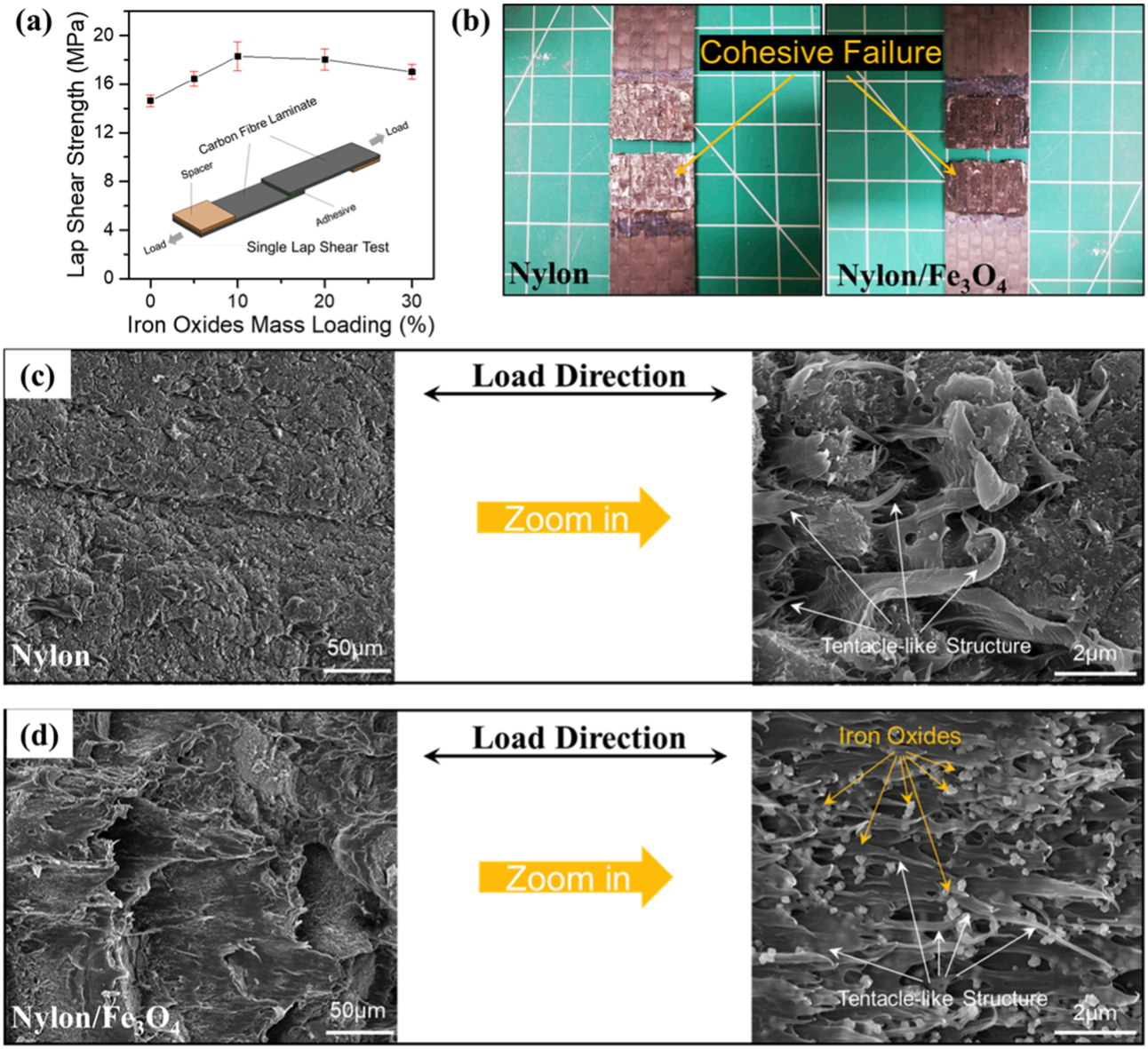

Fig. 7. Single lap shear test: (a) plot of lap shear strength against the mass loading of iron oxides; (b) cohesive failure mode in fracture surfaces of nylon and nylon/Fe_3O_4 samples; SEM image about fracture surface of (c) nylon and (d) nylon/Fe_3O_4 samples.

working frequency.

3.4. Finite element modelling

A Finite element (FE) model to predict the heating performance of nanocomposite adhesives was developed with a multiphysics software COMSOL by using its "Heat Transfer in Solids" module. The three-dimensional CAD model of the electromagnetic heating configuration developed for the FE analysis is shown in Fig. 6a. The FE model was meshed using free tetrahedral elements with a predefined fine level element size. A hollow cylinder is used to represent an eight-turn coil with an electrical conductivity of 6×10^7 S/m. A water-cooling system with a flow rate of 0.1 kg/min was added inside the hollow tube of the coil to ensure consistency with the experimental conditions. The around air was set to be stationery with an initial temperature of 20 °C, and the heat transfers in terms of convection and radiation were not considered during the simulation process. A 300 μm thick film representing the nylon adhesive was placed at 2 mm above the spiral coil. Fig. 6b shows the computational results of the magnetic flux distribution under an induction current of 300 A at 189 kHz. The maximum magnetic flux density around the coil is calculated to be 0.07 T, confirming the value quoted in the manual of the induction heating system (EASYHEAT). The magnetic flux density at the adhesive has been obtained from the computational model to around 0.035 T in the centre of adhesive.

The imaginary part μ" of the relative permeability of the nanocomposite adhesive was determined using a simple linear model based on the volume fraction of the magnetic nanoparticles; the μ" pure Fe_3O_4 was reported to be 6×10^{-2} at 200 kHz [33] while the nylon was considered to have zero imaginary permeability:

$$\mu''_{Adhesive} = V_{Fe_3O_4} \times \mu''_{Fe_3O_4} \tag{2}$$

where V_{Fe3O4} denotes the volume fraction of iron oxide nanoparticles. Other modelling parameters such as the density ρ, heat capacity c, and thermal conductivity k are also calculated based on the volume fraction of iron oxide nanoparticles and can be found in Table 1, properties of iron oxides are obtained from ref. [15].

Generally, the applied magnetic field and the real and imaginary components of the complex permeability can be used to express the magnetic flux inside a ferrimagnetic material, as shown in Equation (3):

$$B = \mu_0(\mu' - i\mu'')H \tag{3}$$

where B is the magnetic flux density, μ_0 refers to the vacuum permeability, and H is the magnetic field strength. The power stored and lost in the material are defined by the real part μ' and the imaginary part μ" of the relative permeability, respectively. The hysteresis loss power P equals to the integral area of the B-H curve and can be expressed as [34],

$$P = \oint fBdH = \pi H_p^2 \mu_0 \mu'' f \tag{4}$$

where H_p denotes the peak magnetic field strength, and f the frequency of alternating magnetic field.

It has been reported that ferrimagnetic nanoparticles can achieve higher μ" in a liquid medium than in a solid matrix due to the rotation and alignment of the ferrimagnetic nanoparticles in a liquid subjected to an alternating magnetic field [32]. Therefore, when a polymer nanocomposite film is heated to above its melting point, its imaginary part of the magnetic permeability will change correspondingly as the iron oxide nanoparticles are more easily to be aligned under magnetic field in liquid state substrate. As the initial heating rate of adhesive film can be expressed in terms of the heating power and the heat capacities, a higher μ" results in a larger energy dissipation that in turn yields a higher heating rate. According to the following equation from ref. [15],

$$k = \frac{dT}{dt} = \frac{P}{c_p} = \frac{\pi V_{Fe_3O_4} \mu_0 \mu''_{Fe_3O_4}}{c_p} H_p^2 f \tag{5}$$

where k is the initial heating rate, and c_p is the volumetric specific heat capacity of the adhesive, P, H_p, V_{Fe3O4}, f, μ_0 and μ'' in Eq. (5) carry the same meaning as in Eq. (2) and Eq. (4). Adopting the higher value of μ" for aligned nanoparticles by multiply a factor based on the measured heating rate increasing ratio in Fig. 5d, the heating performances of aligned adhesives are simulated and compared with the experimental results. Fig. 6c shows an example of stable temperature results of the nylon/20 wt% Fe_3O_4 adhesive before and after the magnetic aligning under an induction current of 300 A. The model predictions match well with those obtained from experiments, as shown in Fig. 6d.

3.5. Bonding strength

Single lap shear tests were conducted to characterize the bond strength of the nanocomposite adhesives with different concentrations of nanoparticles. A typical single lap shear test specimen is presented in Fig. 7a together with the shear strength results. The un-modified nylon adhesive can achieve a lap shear strength of 14.6 MPa (SD = 0.47 MPa), which is 78% higher than the highest strength of EMAA (8.2 MPa) [15], indicating that nylon 12 is a significantly stronger candidate for reversible bonding. The single lap shear test results reveal the lap shear strength of the nanocomposite adhesive increased initially but then decreased with the concentration of the magnetic nanoparticles. The maximum lap shear strength (18.28 MPa, SD = 1.19 MPa) was achieved with 10 wt% magnetic nanoparticles, about 25.3% higher than that of pristine nylon adhesive. It is noted that the lap shear strength results presented in Fig. 7a are all from unaligned original adhesives. An independent samples T-test were conducted to compare the lap shear strength between the original and aligned nylon/10 wt% Fe_3O_4 adhesives to determine the statistical significance. According to T test results, the lap shear strengths of the original nylon/10 wt% Fe_3O_4 adhesive (M = 18.28 MPa, SD = 1.19 MPa) and aligned nylon/10 wt% Fe_3O_4 adhesive (M = 18.17 MPa, SD = 0.84 MPa) were not statistically different ($P = 0.901 > 0.05$). Therefore, the lap shear strengths of the original adhesives can be applied to represent the bonding performance of aligned adhesives, indicating the nanoscale magnetic particle alignment has limited influence on the bonding strength of adhesive. When the magnetic nanoparticles concentration exceeded 10 wt%, the bond strength started to decrease due to the excessive agglomeration of the magnetic nanoparticles [35,36], as can be observed in Fig. S3. Nevertheless, the lap shear strengths of the nanocomposite adhesives remain above that of the un-modified adhesive. The fractured surfaces of joints, as shown in Fig. 7b, show that the failures were all cohesive, indicating excellent bonding between the nanocomposite adhesive and the carbon fibre composites. In contrast, our previous study revealed some interfacial failure between EMAA adhesive and carbon fibre composites [15], which again demonstrate that nylon 12 is a promising candidate for reversible bonding composite structures.

SEM examination of the fractured samples were conducted to investigate the reinforcement effect of magnetic nanoparticles on nylon adhesive. Fig. 7c and 7d show the SEM images of pristine nylon and nylon/Fe_3O_4 samples, respectively. The nylon/Fe_3O_4 samples are seen to exhibit a rougher fracture surface compared with the pristine nylon sample. This rougher surface indicates a higher fracture toughness in nylon/Fe_3O_4 adhesive, which leads to higher lap shear strengths; similar shear strength increase phenomenon was reported by Rao et al. [37] for nanoparticle-filled epoxy nanocomposites. From the high magnification SEM images, it can be observed that there are tentacle-like nylon structures existing on the fracture surfaces, and the directions of those tentacle-like structures are parallel to the load direction of single lap shear test. Iron oxide nanoparticles can be clearly identified from the high magnification SEM image in Fig. 7d, and they exhibited a uniform distribution within the observation area. These iron oxide nanoparticles toughened the nylon adhesive and produced increased number of small sized tentacle-like structures, thus leading to a much larger surface area for effective stress transfer through interfacial interaction between

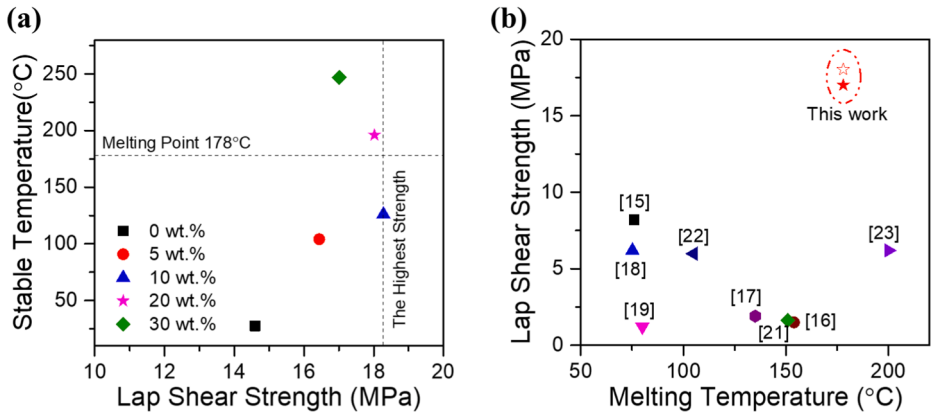

Fig. 8. Performance comparisons: (a) Adhesive performance comparison in terms of stable temperature and lap shear strength; (b) Reference comparison about adhesive's bonding strength.

nylon and iron oxide nanoparticles to provide a higher bonding strength compared with the pristine nylon sample.

Although the nylon/10 wt% adhesive exhibited the highest lap shear strength, the concentration of the magnetic nanoparticles is insufficient to heat the adhesive to above its melting temperature nylon even under the highest induction current used in this study. A comparison was made among the five different nylon adhesives in terms of the stable temperature as well as the lap shear strength, as shown in Fig. 8a. It can be observed that the nylon/20 wt% Fe_3O_4 adhesive can achieve stable temperature above its melting point and a lap shear strength close to the maximum value, suggesting an optimum condition for reversible bonding, i.e., achieving reversible bonding while retaining the high bond strength. It is noteworthy that, despite not exhibiting the highest lap shear strength, the nylon/30 wt% Fe_3O_4 adhesive demonstrates the highest initial heating rate. This characteristic renders it well-suited for applications where rapid heating rates are prioritized over sheer strength. Fig. 8b shows the performance of multiple kinds of adhesives in terms of the lap shear strength and melting temperature, including poly (ethylene-methacrylic acid) (EMAA) [15], commercial polyolefin based hot-melt adhesive (HMA) [16,17], ethylene vinyl acetate (EVA) [18], poly(ethylene-co-butylene) [19], APOA/Polyolefin ester [21], natural rubber [22], and acrylonitrile butadiene styrene (ABS) [23]. It can be clearly observed that the nylon/Fe_3O_4 adhesives developed in this study have effectively filled gaps in the reversible bonding area, particularly as high-strength adhesives with high melting points, which have potential applications in a wider range of areas, including biomedical, electronic reuse, and recycling of bonded structures in the automotive and aerospace industry.

4. Conclusion

In this work, a novel method is presented for creating reversible adhesive by reinforcing Nylon 12 adhesive with Fe_3O_4 nanoparticles. To achieve improved induction heating performance of the reversible adhesive, the Fe_3O_4 nanoparticles within the nylon adhesive were not randomly dispersed, but rather magnetically aligned along the thickness direction of the adhesive using an alternating magnetic field during the hot-melt process. Experimental results show that the pre-aligned nanocomposite adhesives can achieve 200% higher heating rate than the unmodified adhesive. The improvement in the heating performance can be attributed to the aligned nanoparticles featuring a higher imaginary part of the relative permeability μ'' than their un-aligned counterparts, as reported in refs. [32] and [34]. The nano-reinforcement by Fe_3O_4 has been found to improve the bond strength while enabling inductive heating for reversible bonding. The new in-situ alignment technique makes it possible to achieve better inductive heating performance without using excessive Fe_3O_4 nanoparticles that can result in agglomeration of nanoparticles and degradation of the bond strength of the adhesive, paving the way for the development of a high-performance self-heating thermoplastic composite for reversible bonding and self-healing solutions.

CRediT authorship contribution statement

Zhao Sha: Conceptualization, Methodology, Investigation, Validation, Formal analysis, Writing – original draft. **Xinying Cheng:** Conceptualization, Investigation, Software. **Andrew D.M. Charles:** Investigation, Validation, Resources. **Yang Zhou:** Methodology. **Mohammad S. Islam:** Investigation. **Andrew N. Rider:** Resources, Methodology, Funding acquisition. **Shuhua Peng:** Visualization, Funding acquisition, Methodology. **May Lim:** Resources, Methodology. **Victoria Timchenko:** Resources, Methodology, Software. **Chun H. Wang:** Conceptualization, Methodology, Supervision, Formal analysis, Funding acquisition, Investigation, Project administration, Resources, Writing – review & editing.

Declaration of Competing Interest

The authors declare that they have no known competing financial interests or personal relationships that could have appeared to influence the work reported in this paper.

Data availability

Data will be made available on request.

Acknowledgement

This research is Phase 2 of "Adhesives for Structural Joining" topic under the scheme of "A Joint Effort", which is supported by Commonwealth of Australia as represented by Defence Science and Technology (DST Group) and Small Business Innovation Research for Defence (SBIRD), part of the Next Generation Technologies Fund. The authors acknowledge the facilities and the scientific and technical assistance of Microscopy Australia at the Electron Microscope Unit (EMU) within the Mark Wainwright Analytical Centre (MWAC) at UNSW Sydney.

Appendix A. Supplementary data

Supplementary data to this article can be found online at https://doi.org/10.1016/j.compstruct.2023.117304.

References

[1] Chand S. Review Carbon fibers for composites. J Mater Sci 2000;35:1303–13. https://doi.org/10.1023/A:1004780301489.

[2] Zhang T, Meng J, Pan Q, Sun B. The influence of adhesive porosity on composite joints. Compos Commun 2019;15:87–91. https://doi.org/10.1016/j.coco.2019.06.011.

[3] Kupski J, Teixeira de Freitas S. Design of adhesively bonded lap joints with laminated CFRP adherends: Review, challenges and new opportunities for aerospace structures. Compos Struct 2021;268:113923. https://doi.org/10.1016/j.compstruct.2021.113923.

[4] Thoppul SD, Finegan J, Gibson RF. Mechanics of mechanically fastened joints in polymer–matrix composite structures – A review. Compos Sci Technol 2009;69:301–29. https://doi.org/10.1016/j.compscitech.2008.09.037.

[5] Sachse R, Pickett AK, Middendorf P. Analysis of crack-arrest design features for adhesively bonded composite joints: An experimental and numerical study. Compos Struct 2021;274:114301. https://doi.org/10.1016/j.compstruct.2021.114301.

[6] Fame CM, Wu C, Feng P, Tam L. Numerical investigations on the damage tolerance of adhesively bonded pultruded GFRP joints with adhesion defects. Compos Struct 2022;301:116223. https://doi.org/10.1016/j.compstruct.2022.116223.

[7] Khafagy KH, Stoumbos TG, Inoyama D, Datta S, Chattopadhyay A. In-situ investigation of temperature-dependent adhesive properties and failure modes in composite bonded joints. Compos Struct 2022;300:116113. https://doi.org/10.1016/j.compstruct.2022.116113.

[8] Kinloch AJ, Lee JH, Taylor AC, Sprenger S, Eger C, Egan D. Toughening structural adhesives via nano- and micro-phase inclusions. J Adhes 2003;79:867–73. https://doi.org/10.1080/00218460309551.

[9] Lee JS, Kim M, Lee MW. Debonding-on-demand adhesive film using internal Joule heating effect of the steel-aramid braided reinforcement. Compos Struct 2022;286:115290. https://doi.org/10.1016/j.compstruct.2022.115290.

[10] Vattathurvalappil SH, Hassan SF, Haq M. Healing potential of reversible adhesives in bonded joints. Compos Part B Eng 2020;200:108360. https://doi.org/10.1016/j.compositesb.2020.108360.

[11] Croll AB, Hosseini N, Bartlett MD. Switchable Adhesives for Multifunctional Interfaces. Adv Mater Technol 2019;4:1900193. https://doi.org/10.1002/admt.201900193.

[12] Li W, Frederick H, Palardy G. Multifunctional films for thermoplastic composite joints: Ultrasonic welding and damage detection under tension loading. Compos Part A Appl Sci Manuf 2021;141:106221. https://doi.org/10.1016/j.compositesa.2020.106221.

[13] Jongbloed B, Vinod R, Teuwen J, Benedictus R, Villegas IF. Improving the quality of continuous ultrasonically welded thermoplastic composite joints by adding a consolidator to the welding setup. Compos Part A Appl Sci Manuf 2022;155:106808. https://doi.org/10.1016/j.compositesa.2022.106808.

[14] Goh GD, Yap YL, Agarwala S, Yeong WY. Recent Progress in Additive Manufacturing of Fiber Reinforced Polymer Composite. Adv Mater Technol 2019;4:1800271. https://doi.org/10.1002/admt.201800271.

[15] Cheng X, Zhou Y, Charles ADM, Yu Y, Islam MS, Peng S, et al. Enabling contactless rapid on-demand debonding and rebonding using hysteresis heating of ferrimagnetic nanoparticles. Mater Des 2021;210:110076. https://doi.org/10.1016/j.matdes.2021.110076.

[16] Koricho EG, Verna E, Belingardi G, Martorana B, Brunella V. Parametric study of hot-melt adhesive under accelerated ageing for automotive applications. Int J Adhes Adhes 2016;68:169–81. https://doi.org/10.1016/j.ijadhadh.2016.03.006.

[17] Ciardiello R, Belingardi G, Litterio F, Brunella V. Thermomechanical characterization of reinforced and dismountable thermoplastic adhesive joints activated by microwave and induction processes. Compos Struct 2020;244:112314. https://doi.org/10.1016/j.compstruct.2020.112314.

[18] Park Y-J, Joo H-S, Kim H-J, Lee Y-K. Adhesion and rheological properties of EVA-based hot-melt adhesives. Int J Adhes Adhes 2006;26:571–6. https://doi.org/10.1016/j.ijadhadh.2005.09.004.

[19] Heinzmann C, Coulibaly S, Roulin A, Fiore GL, Weder C. Light-Induced Bonding and Debonding with Supramolecular Adhesives. ACS Appl Mater Interfaces 2014;6:4713–9. https://doi.org/10.1021/am405302z.

[20] Salimi S, Babra TS, Dines GS, Baskerville SW, Hayes W, Greenland BW. Composite polyurethane adhesives that debond-on-demand by hysteresis heating in an oscillating magnetic field. Eur Polym J 2019;121:109264. https://doi.org/10.1016/j.eurpolymj.2019.109264.

[21] Verna E, Cannavaro I, Brunella V, Koricho EG, Belingardi G, Roncato D, et al. Adhesive joining technologies activated by electro-magnetic external trims. Int J Adhes Adhes 2013;46:21–5. https://doi.org/10.1016/j.ijadhadh.2013.05.008.

[22] Muzakkar MZ, Ahmad S, Yarmo MA, Jalar A, Bijarimi M. Shear Strength of Single Lap Joint Aluminium-Thermoplastic Natural Rubber (Al-TPNR) Laminated Composite. J Phys Conf Ser 2013;423:12041. https://doi.org/10.1088/1742-6596/423/1/012041.

[23] Vattathurvalappil SH, Haq M. Thermomechanical characterization of Nano-Fe3O4 reinforced thermoplastic adhesives and single lap-joints. Compos Part B Eng 2019;175:107162. https://doi.org/10.1016/j.compositesb.2019.107162.

[24] Li W, Bouzidi L, Narine SS. Current Research and Development Status and Prospect of Hot-Melt Adhesives: A Review. Ind Eng Chem Res 2008;47:7524–32. https://doi.org/10.1021/ie800189b.

[25] Pingkarawat K, Wang CH, Varley RJ, Mouritz AP. Healing of fatigue delamination cracks in carbon–epoxy composite using mendable polymer stitching. J Intell Mater Syst Struct 2014;25:75–86. https://doi.org/10.1177/1045389X13505005.

[26] Li S-L, Wang Y-T, Liu B-W, Shi H-G, Zhao H-B, Wang Y-Z. Fe3O4@PANI/chitosan composite aerogel with electromagnetic induction heating capacity toward efficient removing viscous oil. Compos Commun 2022;36:101367. https://doi.org/10.1016/j.coco.2022.101367.

[27] Sweeney CB, Moran AG, Gruener JT, Strasser AM, Pospisil MJ, Saed MA, et al. Radio Frequency Heating of Carbon Nanotube Composite Materials. ACS Appl Mater Interfaces 2018;10:27252–9. https://doi.org/10.1021/acsami.8b06268.

[28] Barroeta Robles J, Dubé M, Hubert P, Yousefpour A. Repair of thermoplastic composites: an overview. Adv Manuf Polym Compos Sci 2022;8:68–96. https://doi.org/10.1080/20550340.2022.2057137.

[29] Bayerl T, Duhovic M, Mitschang P, Bhattacharyya D. The heating of polymer composites by electromagnetic induction – A review. Compos Part A Appl Sci Manuf 2014;57:27–40. https://doi.org/10.1016/j.compositesa.2013.10.024.

[30] Ciardiello R, Belingardi G, Martorana B, Brunella V. Physical and mechanical properties of a reversible adhesive for automotive applications. Int J Adhes Adhes 2019;89:117–28. https://doi.org/10.1016/j.ijadhadh.2018.12.005.

[31] Sotiriou GA, Visbal-Onufrak MA, Teleki A, Juan EJ, Hirt AM, Pratsinis SE, et al. Thermal Energy Dissipation by SiO2-Coated Plasmonic-Superparamagnetic Nanoparticles in Alternating Magnetic Fields. Chem Mater 2013;25:4603–12. https://doi.org/10.1021/cm402896x.

[32] Yamaminami T, Ota S, Trisnanto SB, Ishikawa M, Yamada T, Yoshida T, et al. Power dissipation in magnetic nanoparticles evaluated using the AC susceptibility of their linear and nonlinear responses. J Magn Magn Mater 2021;517:167401. https://doi.org/10.1016/j.jmmm.2020.167401.

[33] Iwauchi K, Kita Y, Koizumi N. Magnetic and Dielectric Properties of Fe3O4. J Phys Soc Japan 1980;49:1328–35. https://doi.org/10.1143/JPSJ.49.1328.

[34] Tavakoli H, Bormann D, Ribbenfjärd D, Engdahl G. Comparison of a simple and a detailed model of magnetic hysteresis with measurements on electrical steel, COMPEL - Int. J Comput Math Electr Electron Eng 2009;28:700–10. https://doi.org/10.1108/03321640910940954.

[35] Ashraf MA, Peng W, Zare Y, Rhee KY. Effects of Size and Aggregation/Agglomeration of Nanoparticles on the Interfacial/Interphase Properties and Tensile Strength of Polymer Nanocomposites. Nanoscale Res Lett 2018;13:214. https://doi.org/10.1186/s11671-018-2624-0.

[36] Zare Y. Study of nanoparticles aggregation/agglomeration in polymer particulate nanocomposites by mechanical properties. Compos Part A Appl Sci Manuf 2016;84:158–64. https://doi.org/10.1016/j.compositesa.2016.01.020.

[37] Rao Q, Huang H, Ouyang Z, Peng X. Synergy effects of multi-walled carbon nanotube and graphene nanoplate filled epoxy adhesive on the shear properties of unidirectional composite bonded joints. Polym Test 2020;82:106299. https://doi.org/10.1016/j.polymertesting.2019.106299.